Hindawi Publishing Corporation
Paleontology Journal
Volume 2013, Article ID 947839, 17 pages
http://dx.doi.org/10.1155/2013/947839

Research Article

Revision of the Messinian-Early Zanclean Sediments from ODP Hole 953C (Canary Island Archipelago, North-Eastern Atlantic): Biostratigraphy, Cyclostratigraphy, and Astronomical Tuning

Federica Riforgiato

Dipartimento di Scienze della Terra, Università di Siena, Via Laterina 8, 53100 Siena, Italy

Correspondence should be addressed to Federica Riforgiato; riforgiato@gmail.com

Received 4 September 2012; Revised 22 January 2013; Accepted 23 January 2013

Academic Editor: Matías Reolid

A quantitative study was performed on calcareous plankton of the Messinian-early Zanclean succession recovered at ODP Leg 157 Hole 953C (Canary Island Archipelago, North-Eastern Atlantic). This revision allowed to recognize some events typically recorded in the Mediterranean region, highlighting affinities between the Mediterranean and North Atlantic Ocean, in the considered time interval. The presence of such events in an open-ocean succession provides the possibility to substantially improve the biostratigraphic resolution and supplies useful correlation tools between the Mediterranean and oceanic areas. Moreover, to unravel cyclical patterns of deposition and given that the investigated succession shows no evident lithological pattern, cyclostratigraphic analyses have been based on abundance fluctuations of *Globigerinoides-Orbulina* group, neogloboquadrinids, and warm-water versus cool-water species ratio. As a result, forty-three precession-controlled cycles have been recognized spanning from 6.457 Ma to 4.799 Ma.

1. Introduction

The Messinian Salinity Crisis (MSC), affecting the Mediterranean area during the latest Miocene, has been the focus of numerous studies (e.g., [1–18]). It is considered as one of the catastrophic oceanographic events that occurred in the last 20 million years [5, 8, 19]. It was caused by the temporary isolation of the Mediterranean basin from the Atlantic Ocean, due to a combination of tectonic and climatic factors (e.g., [19–21]). According to numerous authors, the onset of the MSC was synchronous over the entire Mediterranean basin and its end corresponded to the catastrophic flooding of marine waters from the Atlantic Ocean (e.g., [19, 20, 22–34]). The sedimentary expression of this flooding is recorded everywhere, both in land sections and in the deep sea cores, showing that the transition from continental to marine environment across Miocene-Pliocene boundary was (i) typified by continuous sedimentation; (ii) geologically instantaneous; (iii) synchronous throughout the Mediterranean basin. However, the problem of the exact timing and origin of the Pliocene flooding of the Mediterranean is not yet completely understood, and the evidence is not irrefutable. Some authors support the early Pliocene flooding of the Mediterranean (e.g., [7, 8, 35]), while others support a late Messinian re-flooding (e.g., [6, 36–41]). Indeed, during the salinity crisis, environmental conditions within the Mediterranean excluded most marine microfossil groups, which are traditionally used for biostratigraphic correlation.

To understand the cause(s) and consequences of the onset of the MSC in detail, an age control is needed for the part of the Atlantic immediately adjacent to the Mediterranean. In this connection, the ODP Leg 157 Hole 953C (Canary Island Archipelago, North-Eastern Atlantic) is considered favourable to the aims of the work for (i) the location; (ii) the excellent paleomagnetic data; (iii) micropaleontological records, despite intervals of no recovery.

Recently, an age control was obtained for the Messinian, both in the Mediterranean and in the low-latitude Atlantic Ocean, through integrated stratigraphic studies complemented by the astronomical tuning of sedimentary cycles or other cyclic variations in continuous marine successions (e.g., [3, 34, 42–52]). Milankovitch cyclostratigraphy is nowadays

considered one of the best tools to gain high-resolution chronostratigraphy in different depositional environments (continental, marginal marine, and deep sea). The presence of high-frequency cycles in deep-sea records and their tuning to the astronomical curve provide an accurate chronology for the stratigraphic events recognized through the studied sedimentary successions. Applications of cyclostratigraphy resulted in the construction of an accurate Astronomical Tuned Neogene Time Scale (ATNTS 2004) for the Quaternary, Pliocene, and late and middle Miocene [3, 42–44, 53–61]. The classic high frequency cyclicity recognized in most of the late Neogene Mediterranean sedimentary record is manifested by the alternation of homogeneous marl and sapropel (or sapropel equivalent) horizons, promoted by astronomical forcing [3]. In this paper, since the succession investigated does not show rhythmic lithological patterns, the proposed cyclostratigraphic reconstruction is mainly based on the quantitative distribution patterns of climate-sensitive planktonic foraminifera taxa (e.g., [62–66]).

The aim of this paper is (i) to present an biostratigraphy for the Messinian-early Zanclean of the Hole 953C, based on quantitative data of planktonic foraminifera (previous studies by [67, 68] are to be considered inadequate for this research); (ii) to compare the bioevents recognized, with those occurring in other astronomically calibrated sections; (iii) to recognize other cyclic patterns for using as further control of the obtained astronomical calibration.

2. Material and Methods

2.1. Site Description. During Ocean Drilling Program Leg 157, four sites (Site 953 to 956; see [70]) were drilled in the volcaniclastic apron of Gran Canaria in the Canary Island Archipelago (North-Eastern Atlantic) (Figure 1). ODP Hole 953C is situated at 28°39′.012N, 15°08′.670W, 68 km northeast of Gran Canaria, 90 km west of Fuerteventura, and 98 km east of Tenerife, at water depth of 3577.8 m. It is the most distally located site on the flanks of Gran Canaria and thus seems to have been spared some of the major slumped intervals and unconformities present at Sites 954, 955, and 956. The recovered sedimentary succession spans the interval from the middle Miocene to Holocene, and the dominant nonvolcanic lithologies were divided into seven major units and three subunits (see [69]). The present study focuses on a 51.11 m thick succession from the Unit III, embracing cores 18R to 13R from 346.89 to 295.78 mbsf (Figure 1) and representing the Messinian-early Zanclean time interval. Core recovery was generally over 50%, and mainly consisting of gray to brownish-gray clayey nannofossil ooze, interbedded with minor graded nannofossil clay-silt, foraminifer lithic silt and sands, and foraminifer sands.

2.2. Sample Preparation and Micropaleontological Analysis

2.2.1. Foraminifera. Samples for foraminiferal analysis were disaggregated in normal water and washed through a 63 μm sieve. The residues were oven dried at 40°C. Qualitative and quantitative planktonic foraminiferal analyses were performed, using a stereoscopic microscope, on 170 samples (average spacing 20 cm). The samples were divided with a microsplitter to obtain unbiased aliquots with about 300 planktonic foraminifera. They were (1) picked, (2) mounted onto faunal slides, (3) determined at specific and supraspecific level, and (4) counted (200–300 specimens) from the larger than 125 μm fraction of the washed residue to collect quantitative faunal data. The assemblages are usually abundant and generally well preserved, although at times they are poor. Very few samples show a very scarce faunal content.

Raw data of microfossils were transformed into percentages over the total abundance, and percentage abundance curves were plotted. Species with phylogenetic affinities and similar environmental significance were also grouped to better interpret distribution patterns.

Furthermore, a semiquantitative analysis from the larger than 63 μm fraction was carried out on all samples in order to pinpoint the actual position of the bioevents.

Benthic foraminifera were also counted to determine plankton/benthos ratio, which is expressed as $\%P = 100 * [P/(P + B)]$ (e.g., [71]).

2.2.2. Calcareous Nannofossil. Standard smear-slides were prepared for the nannofossil analyses for the intervals encompassing the principal bioevents (from core 17R Section 3 to core 13R Section 5). Qualitative analyses on a total of 30 samples have been performed by Dr. Baldassini N (Siena University) to determine additional biohorizons and bioevents to improve the biostratigraphic resolution.

3. Micropaleontological Data

The analysis of the planktonic foraminiferal fauna allowed the identification of 45 taxa, which sometimes were grouped into categories on the basis of morphological, phyletic, or ecological affinities. The categories are (Table 1) *Dentoglobigerina* gr. (*D. altispira altispira*, *D. altispira globosa*), *Globigerinita* gr. (*G. glutinata*, *G. uvula*), *Globigerinoides obliquus* gr. (*G. bollii*, *G.* cf. *elongatus*, *G. emeisi*, *G. extremus*, *G. obliquus*), *Globigerinoides quadrilobatus* gr. (*G. quadrilobatus*, *G. trilobus*, *G. sacculifer*), *Globoturborotalita decoraperta* gr. (*G.* cf. *apertura*, G. *decoraperta*), *Globorotalia menardii* gr. (*G. menardii*, *G. multicamerata*), *Neogloboquadrina* gr. (*N. acostaensis*, *N. pachyderma*, *N. dutertrei humerosa/N. dutertrei blowi*), *Orbulina* gr. (*O. bilobata*, *O. suturalis*, *O. universa*), and *Sphaeroidinellopsis seminulina* gr. (*S. seminulina paenedehiscens*, *S. seminulina seminulina*). Most of the categories are self-explaining, but the labelling of some of them needs further explanation.

Figure 2 shows the quantitative distribution of those species (or categories) which generally display frequencies higher than 1.5%. The main components are *Globoturborotalita nepenthes* and *Neogloboquadrina* gr. which are continuously present throughout the investigated interval, reaching maxima frequencies of 90% and 80%, respectively.

Neogloboquadrina gr. includes also small-sized specimens, sometimes under poor preservation conditions that were difficult to distinguish. Different coiling directions of

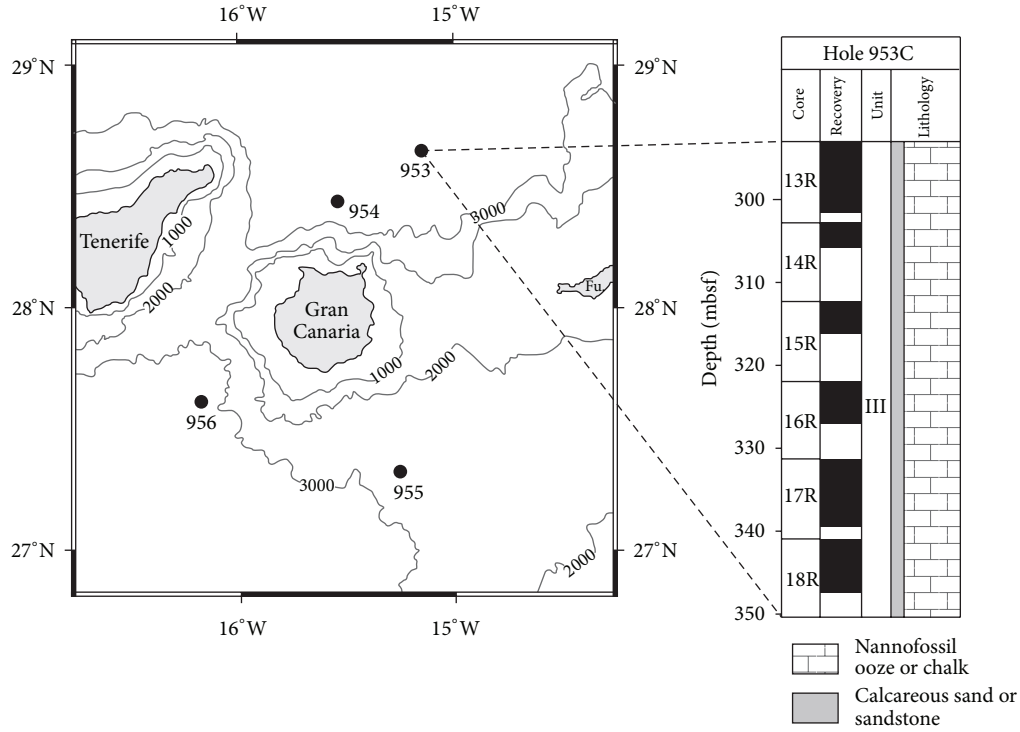

Figure 1: Location map of the ODP Leg 157 Sites 953–956 (Canary Islands) and simplified lithology of Site 953C based on the site description taken from Shipboard Scientific Party [69].

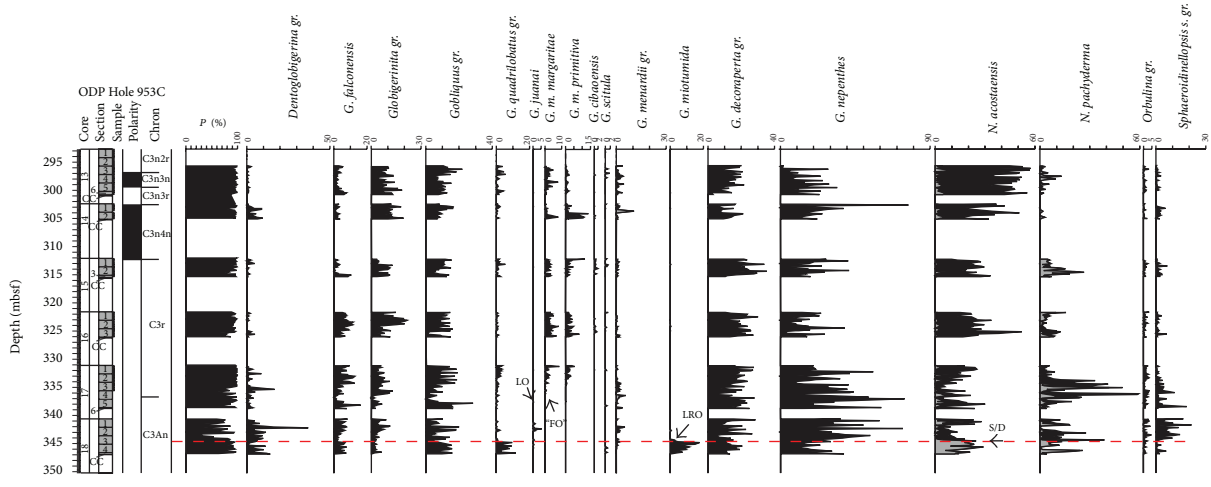

Figure 2: ODP Hole 953C abundance curves of selected planktonic foraminiferal (as a percentage of the total planktonic foraminiferal fauna) and position of most significant biohorizons. Grey color in *Globorotalia menardii* gr., *Neogloboquadrina acostaensis,* and *N. pachyderma* distributions indicates the percentage of sinistral forms. The red dotted line designates the hiatus. The following acronyms indicate bioevents: LO (Last Occurrence), FO (First Occurrence), LRO (Last Regular Occurrence), and S/D (sinistral/dextral coiling change).

the *N. acostaensis* (average value of 17%) have been counted separately as far as the study time interval coiling-change of this species has been proved to have potential biostratigraphic significance. Particularly, in the lower part of the studied interval, sinistrally coiled specimens prevail up to 344.57 mbsf, and after this level the dextrally coiled increases in abundance.

N. pachyderma comprises specimens with low trochospiral test, four to five and one-half chambers in the final whorl with the last chamber irregular often a kummerform, surface characterized by large euhedral calcite crystals, umbilicus from closed to open but always narrow, and aperture umbilical-extraumbilical with a thick apertural rim. This species is present from the base of the investigated

Table 1: ODP Hole 953C planktonic foraminiferal groups used for the quantitative analyses.

Dentoglobigerina altispira altispira	*Dentoglobigerina* group
Dentoglobigerina altispira globosa	
Globigerinita glutinata	*Globigerinita* group
Globigerinita uvula	
Globigerinoides bollii	*Globigerinoides obliquus* group
Globigerinoides cf. *elongatus*	
Globigerinoides emeisi	
Globigerinoides extremus	
Globigerinoides obliquus	
Globigerinoides quadrilobatus	*Globigerinoides quadrilobatus* group
Globigerinoides sacculifer	
Globigerinoides trilobus	
Globorotalia menardii	*Globorotalia menardii* group
Globorotalia multicamerata	
Globoturborotalita cf. *apertura*	*Globoturborotalita decoraperta* group
Globoturborotalita decoraperta	
Neogloboquadrina acostaensis	*Neogloboquadrina* group
Neogloboquadrina dutertrei humerosa/dutertrei blowi	
Neogloboquadrina pachyderma	
Orbulina bilobata	*Orbulina* group
Orbulina suturalis	
Orbulina universa	
Sphaeroidinellopsis seminulina paenedehiscens	*Sphaeroidinellopsis seminulina* group
Sphaeroidinellopsis seminulina seminulina	

interval showing abundances of about 30% with peaks of abundance in the range of 40%–60%. The coiling direction of *N. pachyderma* is prevalently sinistral.

N. dutertrei humerosa/*N. dutertrei blowi* (following the concept of [72]) comprises specimens showing low trochospiral test with five or more chambers in final whorl, surface uniformly moderately perforate with the characteristic rosette pattern formed by concentric arrangement of euhedral crystals on each chamber, umbilicus open and deep, aperture umbilical-extraumbilical, and a moderately high arch bordered by a distinct rim (in *N. dutertrei humerosa*). *N. dutertrei humerosa*/*N. dutertrei blowi* first occurs at 336.47 mbsf displaying low percentage value about 2.6%. The coiling direction of this phenotypic couple is prevalently sinistral.

G. decoraperta gr. and *G. obliquus* gr. show a continuous presence along the investigated interval with high abundance value of approximately 35.5% and 33%, respectively.

Dentoglobigerina gr. displays low frequencies (average value of 2.1%) intervals with isolated abundance peaks higher than 15%.

Sphaeroidinellopsis seminulina gr. shows a general trend very similar to that of *Dentoglobigerina* gr., displaying low values (approximately 2%) but a continuous distribution with peaks of abundance higher than 14%.

Keeled globorotalids are represented by *Globorotalia miotumida*, *G. menardii* gr., *G. margaritae margaritae,* and *G. cibaoensis*.

G. miotumida, which includes less inflated forms, is present from the bottom of the studied interval with low frequencies (average value of 7%) up to 344.35 mbsf where it disappears. From this depth three short influxes are recorded (average value of 0.5%). The coiling direction of *G. miotumida* is prevalently sinistral.

G. menardii gr. includes the species *G. menardii* and *G. multicamerata*. *G. menardii* shows low and scattered occurrence from the base of the investigated interval (average value of 1.3%). The coiling direction is prevalently dextral with short sinistral influxes. *G. multicamerata*, which includes the forms with seven to ten chambers in the final whorl, first occurs at 342.05 mbsf and displays a low a discontinuous distribution with a maximum of approximately 2%. Throughout the studied interval, it is exclusively dextral.

G. margaritae margaritae occurs firstly at 336.11 mbsf, displaying a continuous presence until the top of the studied interval with low percentage value (about 9%). The coiling direction of this species is prevalently sinistral.

G. cibaoensis first occurs at 325.25 mbsf, showing low (about 2%) and scattered distribution up to 297.28 mbsf where it disappears. Throughout the studied interval, it is prevalently sinistral.

Unkeeled globorotalids are represented by *Globorotalia juanai*, *G. margaritae primitiva,* and *G. scitula*. *G. juanai* is present from the base of the investigated interval, showing abundance of about 5% that decreases until its disappearance at 337.66 mbsf.

G. margaritae primitiva first occurs at 337.49 mbsf, displaying low but continuous distribution (about 9%) with isolated abundance peaks higher than 10%. Throughout the studied interval, it is exclusively sinistral.

G. scitula shows low (about 1.4%) and scattered occurrences from the base. The coiling direction of this species is exclusively dextral.

Additional and significant taxa such as *Globigerina falconensis* (about 16%), *Globigerinita* gr. (about 22%), *G. quadrilobatus* gr. (about 14%), *Orbulina* gr. (about 5%), and *Sphaeroidinellopsis seminulina* gr. (about 21%) are continuously present throughout the investigated interval.

Table 2: ODP Hole 953C calcareous plankton bioevents. The asterisk indicates that the bioevents occur within the hiatus, which is an age span about 6.436 to 6.252 Ma.

	Bioevents	Samples	mbsf	Chron	Age (Ma)
10	*Amaurolithus bizzarus* First Occurrence	14R-2, 10–12 cm	304	C3n.4n	5.038
9	*Triquetrorhabdulus rugosus* Last Occurrence	15R-2, 63–65 cm	312.73	C3r	5.244
8	*Neogloboquadrina acostaensis* first influx sx	15R-2, 95–97 cm	314.55	C3r	5.297
7	*Helicosphaera stalis ovata* Last Occurrence	16R-3, 91–93 cm	325.78	C3r	5.681
6	*Nicklithus amplificus* Last Occurrence	17R-3, 42–44 cm	334.52	C3r	5.979
5	*Globorotalia margaritae margaritae* First Occurrence	17R-4, 51–53 cm	336.11	C3An	6.017
4	*Globorotalia juanai* Last occurrence	17R-5, 56–58 cm	337.66	C3An	6.058
3	*Globorotalia miotumida* Last Occurrence	18R-3, 75–77 cm	344.35	C3An	*
2	*Globorotalia miotumida* Last Regular Occurrence	18R-3, 96.5–98.5 cm	344.57	C3An	*
1	*Neogloboquadrina acostaensis* coiling change	18R-3, 96.5–98.5 cm	344.57	C3An	*

4. Biostratigraphy

Calcareous plankton biostratigraphy of the Hole 953C is based on the stratigraphic distribution of several Late Miocene-early Pliocene marker species. Ten biostratigraphic events, which have previously been dated astronomically both in the Atlantic Ocean and in the Mediterranean Sea, are also recognized in this work.

In the following, distribution patterns of the main biostratigraphic marker species are discussed in detail and compared with other land or deep-sea successions both from the Mediterranean Sea and Atlantic Ocean. The first, last regular, and last occurrences (FO, LRO, and LO) are shown in Table 2.

4.1. Planktonic Foraminifera

4.1.1. Neogloboquadrina acostaensis Coiling Change. The *Neogloboquadrina acostaensis* coiling change is defined by the first common occurrence of dextral forms after a long period of dominance of sinistrally coiled specimens. It has recorded in the preevaporite marls of many Mediterranean sections (e.g., [45, 52, 73, 75–86]) and in the Atlantic Ocean successions (e.g., [48, 82, 87–100]), slightly predating the onset of the latest Miocene glaciation [8, 45, 52, 94, 95, 101, 102]. This event always seems to be located within subchron C3An.1r [84, 97, 103]; it usually occurs prior to the disappearance of *Globorotalia miotumida* ([82] and reference therein), and it is astronomically dated at 6.358 Ma in the Mediterranean area and at 6.373 Ma in the Atlantic one [56]. At Hole 953C, a very prominent sinistral to dextral coiling change of *N. acostaensis* (Plate 1, Figures 5(1), 5(2a), 5(2b), and 5(2c)), is recognized at 344.57 mbsf (sample 157-953C-18R-3, 96.5–98.5 cm). Moreover, this event is followed by pronounced sinistral influxes of the group: twelve in Ain el Beida section [48], while Benson and Rakic-El Beid [98] only recognized five influxes, which are most likely related to a lower sample resolution: two sinistral influxes in Falconara section [52] and in Sorbas Basin [45]. All influxes are located within subchron C3An.1n. In the ODP Hole 953C, five sinistral influxes are recognized between 341.60 and 332.80 mbsf.

Above the last sinistral shift, the coiling of *N. acostaensis* remains dominantly dextral up to the late part of Chron C3r, where a sinistral coiling change of this taxon is recognized at 314.55 mbsf (sample 157-953C-15R-2, 95–97 cm). The presence of this event, referred as "first Pliocene *N. acostaensis* sinistral shifts," is identified both in the Atlantic and in the Mediterranean succession (e.g., [25, 28, 29, 33, 34, 53, 66, 99]).

4.1.2. Last Regular Occurrence and Last Occurrence of Globorotalia miotumida. Globorotalia miotumida is a typical Late Miocene species, recorded in the Mediterranean area (e.g., [45, 52, 73, 78, 93, 105, 106]) and in the Atlantic Ocean successions (e.g., [48, 87, 89, 92, 96, 107, 108]) playing a key role in the correlations between the two areas. At Hole 953C, *G. miotumida* (Plate 2, Figures 6(10a), 6(10b), 6(12a), 6(12b), and 6(12c)) is represented by a rich population from the bottom, up to 344.57 mbsf (sample 157-953C-18R-3, 96.5–98.5 cm) where it realizes the LRO. In the overlying samples, *G. miotumida* becomes rare up to its LO. The last typical specimens were found at 344.35 mbsf (sample 18R-3, 75–77 cm).

According to the literature, these events directly postdate the sinistral to dextral coiling change of *N. acostaensis*. In the Atlantic Ocean, they have been recorded within subchron C3An.1r; the LRO in the Ain el Beida section was found in the range of 6.308–6.311 Ma [48]. In the Mediterranean area, these events occur in the upper part of subchron C3An.2n; at Falconara section the LO was found at 6.506 Ma [52] and at 6.51 Ma by Blanc-Valleron et al. [73], the LRO in the Sorbas Basin at 6.504 Ma [45].

The progressively restricted connection between the Atlantic and Mediterranean during the Messinian was probably responsible for the earlier disappearance of this species from the Mediterranean.

Based on the previously mentioned micropaleontological observations, (i) the change in coiling direction of *N. acostaensis* from left to right (6.37 Ma, [56]) and (ii) the LRO of *G. miotumida* (6.31 Ma, [48]) occurred in the same level. It follows that a hiatus is recorded in the Hole 953C at 344.57 mbsf with an age span about 6.436 Ma to 6.252 Ma. According to Brunner et al. [67], the top of Chron C3An.2n

(6.436 Ma, [56]) and the base of Chron C3An.1n (6.252 Ma, [56]) were apparently removed by slumping.

4.1.3. First Occurrence of Globorotalia margaritae margaritae. The First Occurrence of *Globorotalia margaritae margaritae* has been more widely disputed, because of the taxonomical problems related to its identification near the evolutionary transition from its ancestor.

It has been commonly used as marker for the early Pliocene in the Mediterranean (e.g., [75, 76, 109–113]), in the South Atlantic [114, 115] and in the South Pacific [116–118]. Also, it was found in the uppermost Miocene of the Mediterranean [98]; North Atlantic [48, 82, 98, 119] and Eastern Atlantic [91, 92] within subchron C3An.1r (immediately above to disappearance of *Globorotalia miotumida* in the North Atlantic; [82]), while Benson et al. [97] reported the *G. margaritae* FO in the middle of C3An.2n in both Ain el Beida and Salè cores. Moreover, Saito et al. [120] recorded this event within subchron C3An.1n in the Western Atlantic off Florida, equatorial Pacific, and equatorial Indian Ocean.

This event is astronomically dated at 6.08 Ma [56]. At Hole 953C *G. m. margaritae* (Plate 2, Figures 6(7a), 6(7b), 6(8a), 6(8b), and 6(8c)) occurs firstly at 336.11 mbsf (sample 17R-4, 51–53 cm), but probably it is not the evolutive appearance of the taxon due to the underlying hiatus.

Additional bioevent has been also recognized in the *Globorotalia juanai* LO at 337.66 mbsf, which was recorded in the Ain el Beida section in AEB 29 cycle by Krijgsman et al. [48].

4.2. Calcareous Nannofossils

4.2.1. Last Occurrence of Nicklithus amplificus. The importance of the Last occurrence of *Nicklithus amplificus* as a biostratigraphic marker in the upper Miocene and its reliability for time stratigraphic correlation has been confirmed in studies of numerous deep-sea succession [8, 121–123]; the LO was found at 5.978 Ma in the ODP Site 925 and 926 ([124] and reference therein), at 5.939 Ma in the eastern Mediterranean ([124] and reference therein) and in the age range of 5.972–5.975 Ma in the Ain el Beida section [48]. This event occurs very close to the C3An/C3r Chron boundary and marks the beginning of the Messinian Salinity Crisis [8] in the Mediterranean basins. In the Hole 953C, the LO of this species is recorded at 334.52 mbsf (sample 157-953C-17R-3, 42–44 cm).

4.2.2. Last Occurrence of Triquetrorhabdulus rugosus. The Last Occurrence of *Triquetrorhabdulus rugosus* is traditionally used for identifying the Miocene/Pliocene boundary in open ocean areas and is considered an additional event to recognize the CN10a/CN10b subzonal boundary [125]; it is astronomically dated at 5.279 Ma and at 5.255 Ma in the low-latitude Atlantic [124] and in the Loulja section [34], respectively. In the Mediterranean basin, the *T. rugosus* LO is not considered a useful biostratigraphic event, because it is too rare in the samples. Nevertheless, it was identified in several successions just below the base of the Thvera subchron, and this bioevent is astronomically dated at 5.279 Ma [25, 32, 124, 126–129]. According to the paleomagnetic stratigraphy, *T. rugosus* LO has a closely comparable stratigraphic position in Atlantic and Mediterranean records, and it can be used to correlate the base of the Pliocene in its type area (Eraclea Minoa section—Sicily, [130]) to the oceanic record. At Hole 953C, the LO of this species occurred at 312.73 mbsf (samples 157-953C-15R-2, 63–65 cm).

Two additional bioevents have been also recognized: (i) the *Helicosphaera stalis ovata* LO at 325.78 mbsf (sample 157-953C-16R-3, 91–93 cm) that was recorded in the Ain el Beida section between AEB38 and AEB 39 cycles by Krijgsman et al. [48] and the (ii) *Amaurolithus bizzarus* FO at 304 mbsf (sample 157-953C-14R-2, 10–12 cm), astronomically dated at 5.033 in the Loulja section by van der Laan et al. [34].

5. Cyclostratigraphy and Astronomical Calibration

5.1. Calcareous Plankton as Proxy for Identifying Astronomical Cyclicity. According to Hilgen [54, 55] and Hilgen et al. [3, 43], the high frequency alternations of different lithologies, recognized throughout several Mediterranean land-based sedimentary sequences, have an origin related to the astronomical forcing. For example, the limestone-marl couplets which characterize the Lower Pliocene pelagic sediments ("Trubi Fm." *Auct.*, Sicily), reflect the periodicity of the Earth's precession cycle (e.g., [53–55, 127, 128]). The marls were considered as the "equivalent" of the sapropels characterizing higher stratigraphic levels ("M. Narbonne Fm." *Auct.*, Sicily). On this assumption, Hilgen [54, 55] proposed his astronomically calibrated time scale, where marl layers (sapropel equivalents) are correlated to insolation maxima/precession minima and limestones correspond to periods of higher productivity induced by minima of the insolation curve (precession maxima).

In the absence of an evident lithological rhythm, biotic proxies may be taken into account to highlight the astronomical cyclicity of a sedimentary succession. In this framework, cyclostratigraphy and astronomical tuning to the ATNTS [56] has been carried out by means of foraminifera-based proxies (e.g., [62–66, 131, 132]). In particular, the abundances curves of *Globigerinoides/Orbulina* gr., neogloboquadrinids, and the ratio of warm-water versus cool-water species show Milankovitch periodicities. The relationship between selected climate-sensitive planktonic taxa and lithological cyclicity, correlated in turn to astronomical cycles, is well expressed in the lower Messinian deposits of Sicily, Spain, and Greece (Figure 3).

5.1.1. Globigerinoides. In agreement with their unanimously declared warm-climate affinity (e.g., [62–64, 131]), the highest abundances of the *Globigerinoides* population seem to correspond to maxima of the insolation cycles. In the Sicilian "Tripoli Fm." (*Auct.*), consisting of a repetition of the same lithological triplet ("sapropel type" brown laminate-diatomite-marl), high frequencies of *Globigerinoides* gr. concentrate within brown laminates and diatomitic layers,

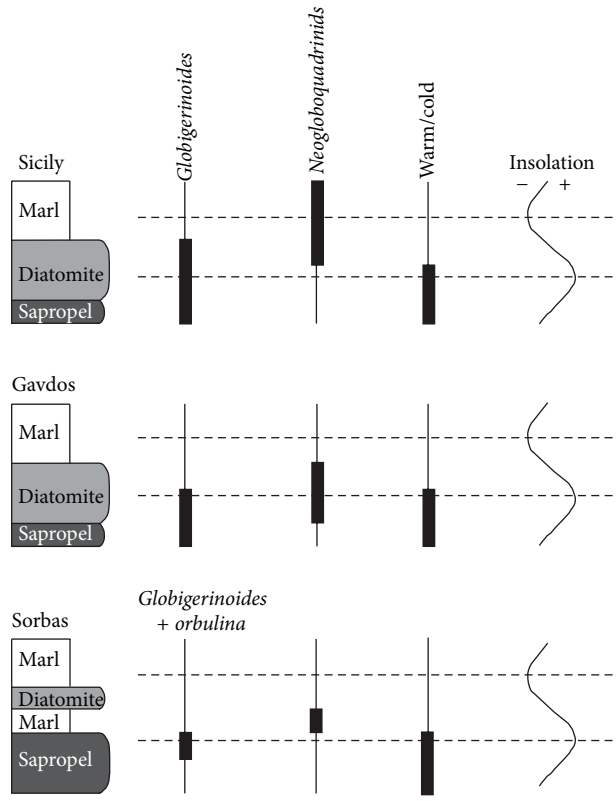

Figure 3: Relationship among astronomically forced lithological cycles, abundances of selected planktonic foraminifera, warm/cold ratio, and inferred insolation cycles in different Mediterranean successions (Sicily; Gavdos Basin—Greece; Sorbas Basin—Spain). (Modified after [73, 74].)

corresponding to insolation maxima [73, 133, 134], whereas lowest frequencies fall within the middle part of the marls. A similar situation is recorded in the coeval sediments of the Gavdos Island (Greece, [45, 46, 74, 135]) where the basic cycle is three-folded as well (sapropel-diatomite-marl). Here, the highest abundances of *Globigerinoides* spp. are recorded within the sapropel and in lower-middle part of the diatomites. In the Sorbas Basin (Southern Spain, [46]), the lower Messinian sediments of the upper Abad section display quadruplet-type lithological cycles (sapropel-marl-diatomite-marl). In this case, maxima abundances of *Globigerinoides* spp. + *Orbulina* spp. are recorded in the middle-upper part of the sapropels or at the transition between the sapropel layers and the first marly horizons (Figure 3).

5.1.2. Neogloboquadrina. Usually reported as cool taxa [136–138], neogloboquadrinids show an evident preference for stratified waters within high-productivity zone associated with the deep chlorophyll maximum (DCM), at the base of the euphotic zone [139–141].

The neogloboquadrinids show maxima frequencies in correspondence of the topmost part of the diatomite and marl layers in the Sicilian Tripoli [73, 134]; they generally reach the highest percentages at the base of the first marl layer in the upper Abad section [46, 142] and within the diatomites at Gavdos [74] (Figure 3), thus implying different parameters than temperature controlling theirs distribution.

5.1.3. Warm/Cold Ratio. The ratio of warm-water versus cool-water taxa using modern habitat characteristics described by Pujol and Grazzini [138], Lourens et al. [53], Pérez-Folgado et al. [74], and Sierro et al. [46] herein follows. Warm-water taxa include *G. decoraperta* gr., *G. quadrilobatus* gr., *G. obliquus*, and *O. universa*, while *Neogloboquadrina* gr., *G. falconensis*, and *G. glutinata* were taken as representative of cool condition.

G. decoraperta gr. (*G. decoraperta* and *G. apertura*) is not living today but its descendant, *G. rubescens*, is currently living in subtropical and tropical environments. This species usually grows in the surface nutrient-depleted waters of the mixed layer in oceanographic settings with a strong stratification in the water column [136, 143, 144].

In the Sorbas basin, this group is abundant in the upper part of the sapropels and the lower part of the diatomites on Gavdos [74].

O. universa behaves as *G. rubescens* in the Sorbas basin and on Gavdos [74].

G. falconensis is a species whose geographic, depth, and seasonal distribution patterns are poorly known, because in the literature it is grouped with *G. bulloides*. However, studies of planktonic foraminiferal assemblages from the western North Atlantic [145], surface sediment data from the South Atlantic [146], and southern Indian Ocean [147] indicate that this species prefers to live in the cool subtropical regions.

G. glutinata is a ubiquitous species living in subarctic to subantarctic waters, low in absolute amount but with a high percentage in waters with very low total foraminiferal concentrations [143]. This species is abundant in the homogeneous marl-sapropel transitions both in the western and eastern Messinian Mediterranean [46, 74].

Generally, planktonic taxa indicative of warm nutrient-poor superficial waters are abundant in sapropels or sapropelitic layers, whereas cold eutrophic deep-water forms characterize the homogeneous marls or the diatomites [46, 73, 102, 148–150].

A close dependence between lithofacies and microfossil assemblages has been proved for sapropel-bearing successions, with by definition, and the same microfossil assemblages can be considered as sensitive to astronomical periodicity also in successions lacking sapropels. Consequently, the abundance variations of the after-mentioned taxa allowed the astronomically tuned with the insolation curve of Laskar et al. ([104], $La04_{1:1}$ solution).

Particularly, insolation maxima-precession minima correspond to (i) maxima in the distribution patterns of both *Globigerinoides*/*Orbulina* gr. and warm/cold ratio; (ii) minima in the distribution patterns of neogloboquadrinids (Figure 4).

5.2. Astronomical Tuning. The magnetic polarity reversal ([67, 70] and reference therein) and the bioevents recognized in the Hole 953C have been used to correlate the studied sedimentary records with Ain el Beida and Loulja sections

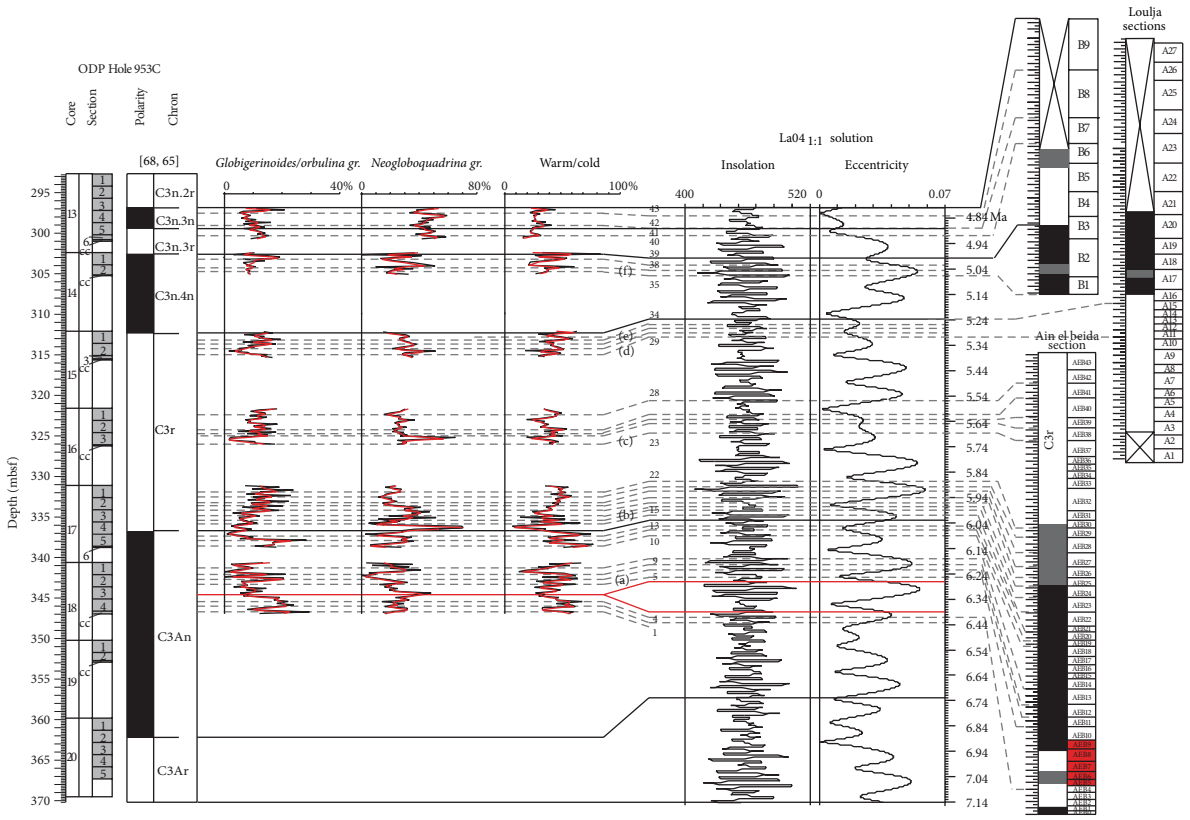

FIGURE 4: Cartoon showing the tuning of the ODP Hole 953C with the insolation and eccentricity curves of $La04_{1:1}$ solution [104] and the correlation to Ain el Beida and Loulja sections ([34, 48], resp.). Grey dotted lines represent the tendency lines of selected taxa and warm/cold ratio curves. The numbers from 1 to 43 refer to the lithological cycles. Position of calcareous plankton bioevents: (a) *Neogloboquadrina acostaensis* coiling change and *Globorotalia miotumida* Last Regular Occurrence; (b) *Nicklithus amplificus* Last Occurrence; (c) *Helicosphaera stalis ovata* Last Occurrence; (d) *N. acostaensis* first influx sx; (e) *Triquetrorhabdulus rugosus* Last Occurrence; (f) *Amaurolithus bizzarus* First Occurrence.

(Morocco), astronomically calibrated by Krijgsman et al. [48] and van der Laan et al. [34], respectively. The sinistral/dextral *N. acostaensis* coiling change, the LO of *N. amplificus*, and the LO of *T. rugosus* are considered synchronous events, which were used as tie points to calibrate astronomically the Hole 953C sedimentary sequence. The S/D *N. acostaensis* and the LO of *N. amplificus* calibrated at 6.378 Ma and 5.975 Ma by Krijgsman et al. [48] and the LO of *T. rugosus* calibrated at 5.255 Ma in cycle LA 15R (and [34]) were used as the starting point for tuning the sedimentary cycles at the Hole 953C. In addition, the LO of *Helicosphaera stalis ovata* LO (recorded in the Ain el Beida section by [48]) and the first sinistral influx of *N. acostaensis* (recorded in Loulja section by [34]) are here considered.

Forty-three sedimentary cycles were recognized in the Hole 953C (Figure 4) and are informally and progressively numbered from the base to the top of the studied interval.

5.2.1. Chron C3An. According to the literature, the Chron C3An (6.733 Ma–6.033 Ma, [56]) comprises thirty-two sedimentary cycles and corresponds to 700 kyrs. At Hole 953C, only thirteen precession cycles (1–13) were recognized due to (i) the 1.92 m thick no-recovery interval in the core 17R, which covers a time interval of 0.088 Ma; (ii) the hiatus identified at 344.57 mbsf with an age span about 6.436 Ma to 6.252 Ma. The cycles are highlighted by positive fluctuations of *Globigerinoides*/*Orbulina* gr.-warm/cold ratio which are in opposite phase respect to the fluctuations of *Neogloboquadrina* gr. Cycles 6 to 8 fit excellently with the high-amplitude fluctuations of the eccentricity curve. According to Krijgsman et al. [48], maxima in eccentricity enhance climate fluctuations on a precessional scale, because the eccentricity modulates the precession amplitude favouring the formation of distinct cycles.

5.2.2. Chron C3r. The Chron C3r (5.235 Ma–6.033 Ma, [56]) comprises a total number of twenty-seven sedimentary cycles and corresponds to 798 kyrs in according to the ATNTS2004 [56]. Twenty precession cycles (14–33) are recognized, owing to the no-recovery interval in the cores 16 (4.86 m thick) and 15 (6.02 m thick) that covers a time interval of 0.1578 Ma and 0.208 Ma, respectively. The cycles are highlighted by the

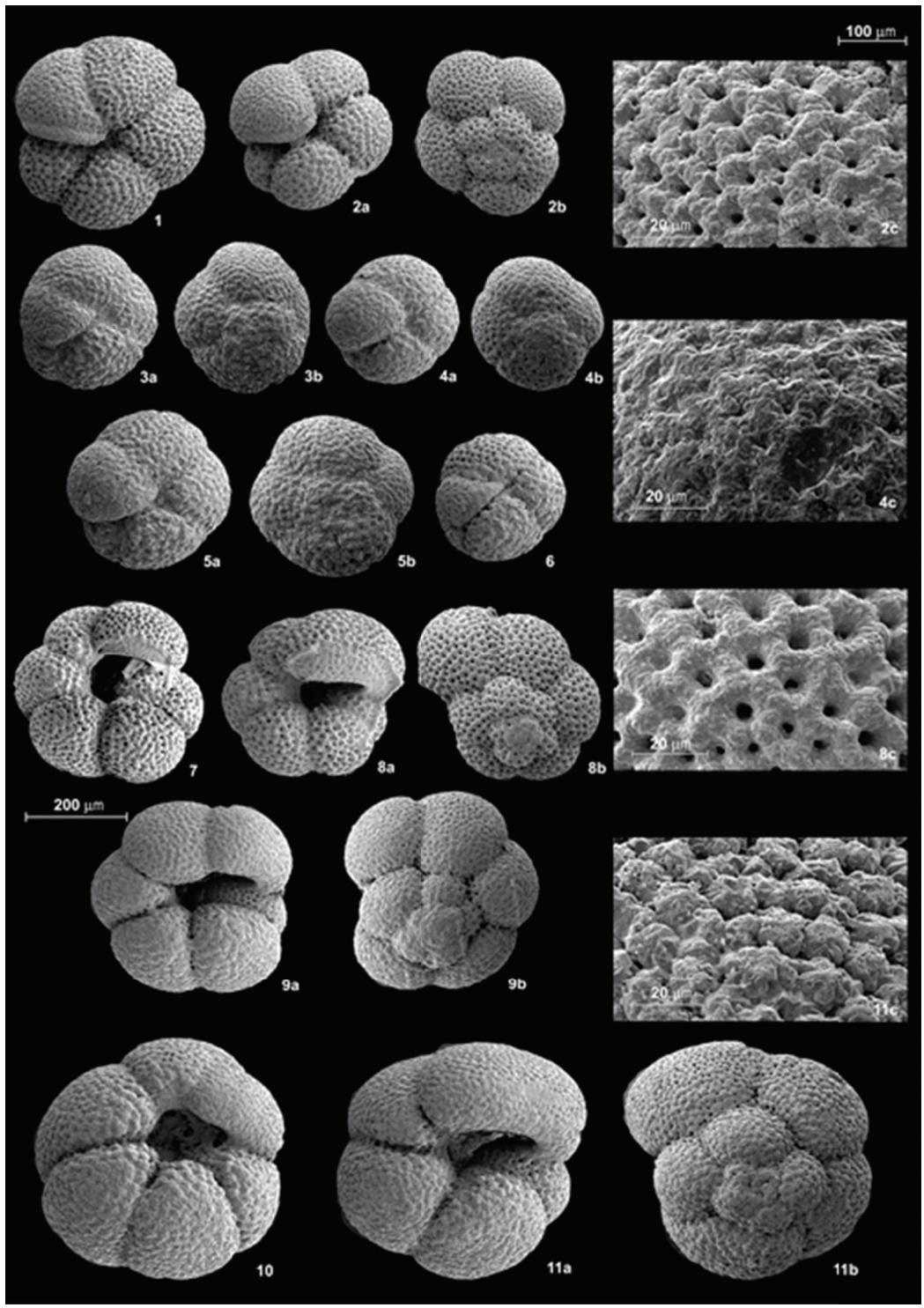

Figure 5

abundance peaks of *Globigerinoides*/*Orbulina* gr.-warm/cold ratio signal, which are in opposite phase with *Neogloboquadrina* gr. distribution (except the cycles 20 and 22). Moreover, cycles 14, 17, and 20 fit excellently with the high-amplitude fluctuations of the eccentricity curve. The increase in thickness of cycles 24 and 27 has been interpreted as a change in the sedimentation rate. Additionally, the cycle 27 is interpreted as "double cycle" due by the fluctuations of the faunal proxies, like cycle AEB 41 from Ain el Beida [48].

In this interval, the recorded bioevents are (i) the LO of *N. amplificus* in the cycle 17 at the astronomical age of 5.979 Ma; (ii) the LO of *H. stalis ovata* in the cycle 24 at the

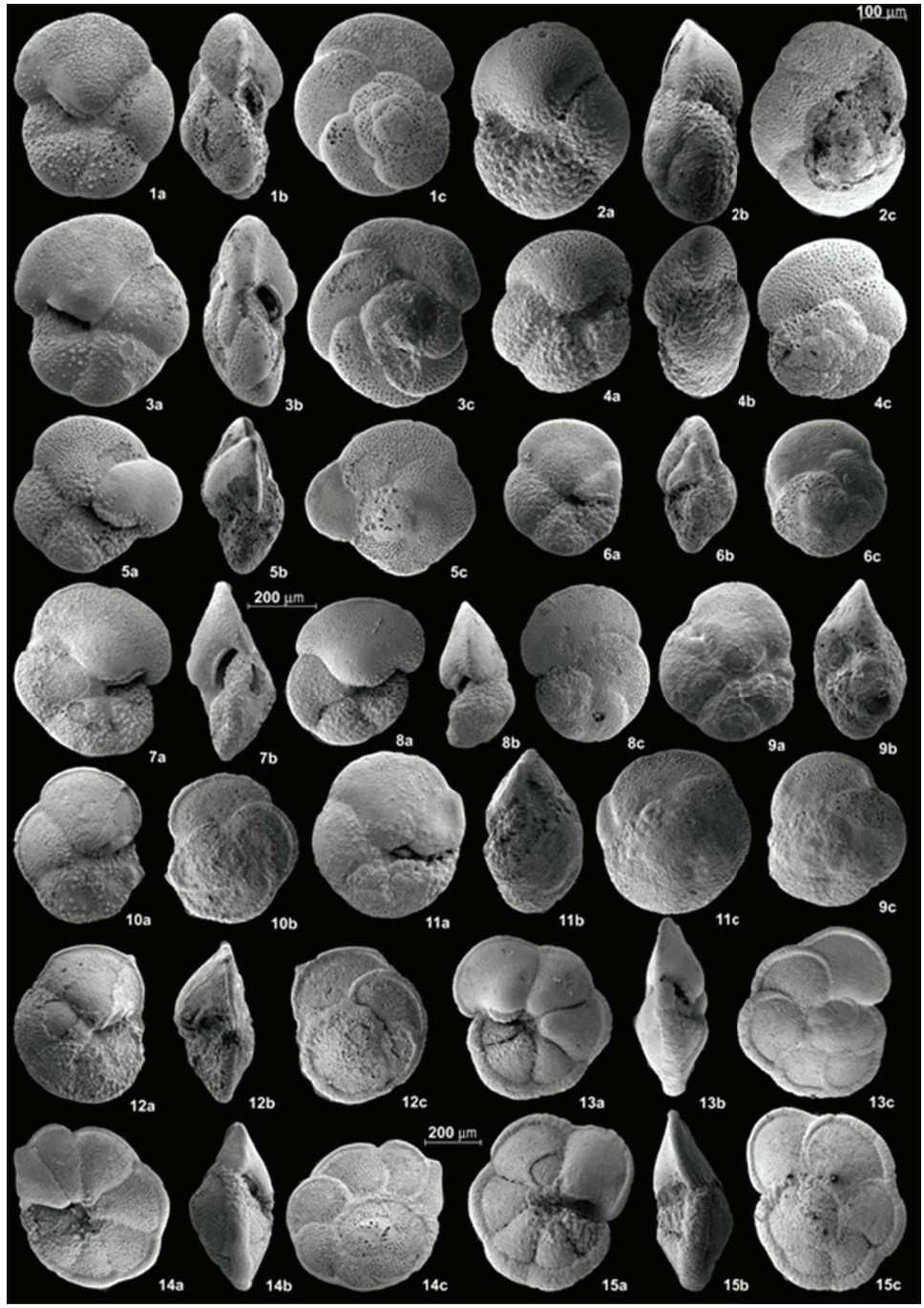

Figure 6

astronomical age of 5.681 Ma; (iii) the presence of *Discoaster quinqueramus* in the cycle 28, which corresponds to cycle AEB 42 of Ain el Beida section [48]; (iv) the first sinistral influx of *N. acostaensis* in the cycle 30 at the astronomical age of 5.297 Ma; (v) the LO of *T. rugosus* in the cycle 33 at the astronomical age of 5.244 Ma. The recognition of these last two bioevents and the base of the Thvera magnetic event are a useful guide to identify the Miocene/Pliocene boundary in the interval studied. Since, from a cyclostratigraphic perspective, the boundary falls within the insolation cycle 510, five precessional cycles below the Thvera magnetic event, and has an astrochronological age of 5.332 Ma [53].

5.2.3. Chron C3n.4n. The Chron C3n.4n (4.997 Ma–5.235 Ma, [56]) comprises a total number of ten sedimentary cycles, corresponding to 238 kyrs according to the ATNTS2004. In this interval, the relation between warm/cold ratio maxima versus neogloboquadrinids minima, allowed

to identified only five precession cycles (35–39), because of no-recovery interval in the core 14 (6.97 m thick) that covers a time interval of 0.12 Ma. In particular, cycles 36-37 fit excellently with the high-amplitude fluctuations of the eccentricity curve. In this interval, the *Globigerinoides*/*Orbulina* gr. signal is not clear or completely absent. In the cycle 37, the FO of *A. bizzarus* is recognized, and it has an astronomical age of 5.038 Ma, corresponding to cycle LB 2R of Loulja section [34].

5.2.4. Chron C3n.3r. In the literature, the Chron C3n.3r (4.896 Ma–4.997 Ma, [56]) comprises a total number of 4.5 sedimentary cycles and corresponds to 101 Kyrs according to the ATNTS2004. Three precession cycles (39–41) are recognized owing to the 1.43 m thick no-recovery interval in the core 13 cover a time interval of 0.044 Ma. The cycles are highlighted by two negative fluctuations of *Neogloboquadrina* gr. that are in opposite phase with those of the warm/cold ratio *Globigerinoides*/*Orbulina* gr. signals. In the cycle 39, the presence of *H. sellii* suggests a correspondence to cycle LB 6 of Loulja section [34].

5.2.5. Chron C3n.3n. In the literature, the Chron C3n.3n (4.799 Ma–4.896 Ma, [56]) comprises a total number of 2.5 sedimentary cycles and corresponds to 97 kyrs according to the ATNTS2004. The cycles (42-43) are highlighted by two negative fluctuations of *Neogloboquadrina* gr., which are in opposite phase with those of the warm/cold ratio *Globigerinoides*/*Orbulina* gr. signals. Finally, the increase in thickness of the cycles has been interpreted as a change in the sedimentation rate.

6. Conclusion

This paper presents the results of qualitative and quantitative analyses of the calcareous plankton assemblages, carried out in tract of the Hole 953C succession encompassing the Messinian to early Zanclean. The study allowed to recognize ten important bioevents, well calibrated and widely used in the Mediterranean and Atlantic correlation. Moreover, a cyclostratigraphic approach has been attempted to obtain a detailed chronostratigraphic subdivision. Lacking any evident lithological cyclicity and the no-recovery intervals along the succession, the combination of climate sensitive records allowed to extract signals of the astronomical cyclicities. The fluctuations curves of *Globigerinoides*/*Orbulina* gr., neogloboquadrinids, and the ratio of warm-water versus cool-water species highlight a frequency indicative of the Earth's precession periodicity. Particularly, the insolation curve is in phase with the *Globigerinoides*/*Orbulina* gr. and warm/cold ratio distribution and is in antiphase with the *Neogloboquadrina* gr. curve. As result, forty-three precession-controlled cycles have been recognized spanning from 6.457 Ma to 4.799 Ma.

Description of Plates 1 and 2

Plate 1 (see Figure 5).

(1) *Neogloboquadrina acostaensis* (Blow): umbilical view, sample 953C-13R-3, 8–10 cm.

(2) *Neogloboquadrina acostaensis* (Blow): (a) umbilical view, (b) spiral view, (c) ultrastructure, sample 953C-13R-3, 8–10 cm.

(3) *Neogloboquadrina pachyderma* (Ehrenberg): (a) umbilical view, (b) spiral view, sample 953C-18R-2, 98–100 cm.

(4) *Neogloboquadrina pachyderma* (Ehrenberg): (a) umbilical view, (b) spiral view, (c) ultrastructure, sample 953C-19R-1, 24.5–26.5 cm.

(5) *Neogloboquadrina pachyderma* (Ehrenberg): (a) umbilical view, (b) spiral view, sample 953C-18R-2, 98–100 cm.

(6) *Neogloboquadrina pachyderma* (Ehrenberg): umbilical view, sample 953C-17R-3, 57–59 cm.

(7) *Neogloboquadrina dutertrei humerosa* (Takayanagi and Saito): umbilical view, sample 953C-13R-2, 140.5–142.5 cm.

(8) *Neogloboquadrina dutertrei humerosa* (Takayanagi and Saito): (a) umbilical view, (b) spiral view, (c) ultrastructure, sample 953C-13R-3, 26–28 cm.

(9) *Neogloboquadrina dutertrei humerosa* (Takayanagi and Saito): (a) umbilical view, (b) spiral view, sample 953C-12R-2, 41.5–43.5 cm.

(10) *Neogloboquadrina dutertrei blowi* Rögl and Bolli: umbilical view, sample 953C-13R-3, 91–93 cm.

(11) *Neogloboquadrina dutertrei blowi* Rögl and Bolli: (a) umbilical view, (b) spiral view, (c) ultrastructure, sample 953C-16R-1, 38–40 cm.

Plate 2 (see Figure 6).

(1) *Globorotalia scitula* (Brady): (a) umbilical view, (b) side view, (c) spiral view, sample 953C-17R-2, 12–14 cm.

(2) *Globorotalia juanai* Bermúdez and Bolli: (a) umbilical view, (b) side view, (c) spiral view, sample 953C-18R-3, 75–77 cm.

(3) *Globorotalia scitula* (Brady): (a) umbilical view, (b) side view, (c) spiral view, sample 953C-14R-2, 45–47 cm.

(4) *Globorotalia juanai* Bermúdez and Bolli: (a) umbilical view, (b) side view, (c) spiral view, sample 953C-17R-5, 108–110 cm.

(5) *Globorotalia margaritae primitiva* Cita: (a) umbilical view, (b) side view, (c) spiral view, sample 953C-17R-1, 80–82 cm.

(6) *Globorotalia margaritae primitiva* Cita: (a) umbilical view, (b) side view, (c) spiral view, sample 953C-17R-2, 138–140 cm.

(7) *Globorotalia margaritae margaritae* Bolli and Bermúdez: (a) umbilical view, (b) side view, sample 953C-16R-3, 74.5–76.5 cm.

(8) *Globorotalia margaritae margaritae* Bolli and Bermúdez: (a) umbilical view, (b) side view, (c) spiral view, sample 953C-13R-4, 147–149.

(9) *Globorotalia cibaoensis* Bermúdez: (a) umbilical view, (b) side view, (c) spiral view, sample 953C-16R-1, 128–130 cm.

(10) *Globorotalia miotumida* Jenkins: (a) umbilical view, (b) spiral view.

(11) *Globorotalia cibaoensis* Bermúdez: (a) umbilical view, (b) side view, (c) spiral view, sample 953C-15R-2, 46–48 cm.

(12) *Globorotalia miotumida* Jenkins: (a) umbilical view, (b) side view, (c) spiral view.

(13) *Globorotalia menardii* (Parker, Jones and Brady): (a) umbilical view, (b) side view, (c) spiral view, sample 953C-16R-2, 144.5–146.5 cm.

(14) *Globorotalia multicamerata* Cushman and Jarvis: (a) umbilical view, (b) side view, (c) spiral view, sample 953C-13R-3, 41.5–43.5 cm.

(15) *Globorotalia menardii* (Parker, Jones and Brady): (a) umbilical view, (b) side view, (c) spiral view, sample 953C-13R-3, 91–93 cm.

For quantitative data of ODP Hole 953C planktonic foraminifera, see Tables 1 and 2 of the Supplementary Material available online at http://dx.doi.org/10.1155/2013/947839.

Acknowledgments

The author is particularly grateful to Gianfranco Salvatorini for discussing data, for his helpful comments, support, and encouragement. She thanks Niccolò Baldassini for calcareous nannoplankton analyses. She is grateful to Hugo Corbí and an anonymous reviewer for their critical reading of the paper. Samples for this study were obtained through the courtesy of the Integrated Ocean Drilling Program. This paper is dedicated to whom is no longer with us and to whom will come soon.

References

[1] W. B. F. Ryan, "Quantitative evaluation of the depth of the western Mediterranean before, during and after the late Miocene salinity crisis," *Sedimentology*, vol. 23, pp. 791–813, 1976.

[2] R. W. H. Butler, W. H. Lickorish, M. Grasso, H. M. Pedley, and L. Ramberti, "Tectonics and sequence stratigraphy in Messinian basins, Sicily: constraints on the initiation and termination of the Mediterranean salinity crisis," *Geological Society of America Bulletin*, vol. 107, no. 4, pp. 425–439, 1995.

[3] F. J. Hilgen, W. Krijgsman, C. G. Langereis, L. J. Lourens, A. Santarelli, and W. J. Zachariasse, "Extending the astronomical (polarity) time scale into the Miocene," *Earth and Planetary Science Letters*, vol. 136, no. 3-4, pp. 495–510, 1995.

[4] J. P. Suc, D. Violanti, L. Londeix et al., "Evolution of the Messinian Mediterranean environments: the Tripoli Formation at Capodarso (Sicily, Italy)," *Review of Palaeobotany and Palynology*, vol. 87, no. 1, pp. 51–79, 1995.

[5] G. Clauzon, J. P. Suc, F. Gautier, A. Berger, and M. F. Loutre, "Alternate interpretation of the Messinian salinity crisis: controversy resolved?" *Geology*, vol. 24, no. 4, pp. 363–366, 1996.

[6] R. Riding, J. C. Braga, J. M. Martín, and I. M. Sánchez-Almazo, "Mediterranean Messinian salinity crisis: constraints from a coeval marginal basin, Sorbas, southeastern Spain," *Marine Geology*, vol. 146, no. 1–4, pp. 1–20, 1998.

[7] W. Krijgsman, F. J. Hilgen, S. Marabini, and G. B. Vai, "New paleomagnetic and cyclostratigraphic age constraints on the Messinian of the Northern Apennines (Vena del Gesso Basin, Italy)," *Memorie della Società Geologica Italiana*, vol. 54, pp. 25–33, 1999.

[8] W. Krijgsman, F. J. Hilgen, I. Raffi, F. J. Sierro, and D. S. Wilson, "Chronology, causes and progression of the Messinian salinity crisis," *Nature*, vol. 400, no. 6745, pp. 652–655, 1999.

[9] M. Roveri, M. A. Bassetti, and F. Ricci Lucchi, "The mediterranean Messinian salinity crisis: an Apennine foredeep perspective," *Sedimentary Geology*, vol. 140, no. 3-4, pp. 201–214, 2001.

[10] M. Roveri, V. Manzi, F. Ricci Lucchi, and S. Rogledi, "Sedimentary and tectonic evolution of the Vena del Gesso basin (Northern Apennines, Italy): implications for the onset of the Messinian salinity crisis," *Geological Society of America Bulletin*, vol. 115, pp. 387–405, 2003.

[11] M. Roveri, S. Lugli, V. Manzi, and B. C. Schreiber, "The Messinian Salinity Crisis: a sequence-stratigraphy approach," *GeoActa, Special Publication*, vol. 1, pp. 117–138, 2008.

[12] J. Lofi, C. Gorini, S. Berné et al., "Erosional processes and paleo-environmental changes in the Western Gulf of Lions (SW France) during the Messinian Salinity Crisis," *Marine Geology*, vol. 217, no. 1-2, pp. 1–30, 2005.

[13] J. Lofi, F. Sage, J. Deverchere et al., "Refining our knowledge of the Messinian salinity crisis records in the offshore domain through multi-site seismic analysis," *Bulletin de la Societe Geologique de France*, vol. 182, no. 2, pp. 163–180, 2011.

[14] V. Manzi, S. Lugli, F. R. Lucchi, and M. Roveri, "Deep-water clastic evaporites deposition in the Messinian Adriatic foredeep (northern Apennines, Italy): did the Mediterranean ever dry out?" *Sedimentology*, vol. 52, no. 4, pp. 875–902, 2005.

[15] F. Sage, G. Von Gronefeld, J. Déverchère, V. Gaullier, A. Maillard, and C. Gorini, "Seismic evidence for Messinian detrital deposits at the western Sardinia margin, northwestern Mediterranean," *Marine and Petroleum Geology*, vol. 22, no. 6-7, pp. 757–773, 2005.

[16] A. Maillard, C. Gorini, A. Mauffret, F. Sage, J. Lofi, and V. Gaullier, "Offshore evidence of polyphase erosion in the Valencia Basin (Northwestern Mediterranean): scenario for the Messinian Salinity Crisis," *Sedimentary Geology*, vol. 188-189, pp. 69–91, 2006.

[17] F. Orszag-Sperber, "Changing perspectives in the concept of "Lago-Mare" in Mediterranean Late Miocene evolution," *Sedimentary Geology*, vol. 188-189, pp. 259–277, 2006.

[18] C. Bertoni and J. A. Cartwright, "Major erosion at the end of the Messinian salinity crisis: evidence from the Levant basin, eastern Mediterranean," *Basin Research*, vol. 19, no. 1, pp. 1365–2117, 2007.

[19] K. J. Hsü, W. B. F. Ryan, and M. B. Cita, "Late miocene desiccation of the mediterranean," *Nature*, vol. 242, no. 5395, pp. 240–244, 1973.

[20] M. B. Cita, R. C. Wright, W. B. F. Ryan, and A. Longinelli, "Messinian paleoenvironments," in *Initial Reports of the Deep Sea Drilling Project*, K. J. Hsü, L. Montadert, D. Bernoulli et al., Eds., vol. 42, pp. 1003–1035, 1978.

[21] K. J. Hsü, L. Montadert, D. Bernouilli et al., "History of the Mediterranean salinity crisis," in *Initial Reports of the Deep Sea Drilling Project*, K. J. Hsü, L. Montadert, D. Bernoulli et al., Eds., vol. 42A, pp. 1053–1078, 1978.

[22] A. Bossio, L. Giannelli, R. Mazzanti, R. Mazzei, and G. Salvatorini, "Gli strati alti del Messiniano, il passaggio Miocene—Pliocene e la sezione plio-pleistocenica di Nugola nelle colline a NE dei Monti Livornesi," in *IX Convegno della Società Paleontologica Italiana*, pp. 55–90, Pacini, Pisa, Italy, 1981.

[23] J. A. McKenzie and R. Sprovieri, "Paleoceanographic conditions following the earliest Pliocene flooding of the Tyrrhenian Sea," in *Proceedings of the Ocean Drilling Program Scientific Results*, K. A. Kastens, J. Mascle, C. Auroux et al., Eds., vol. 107, pp. 405–414, 1990.

[24] A. R. Fortuin, J. M. D. Kelling, and T. B. Roep, "The enigmatic Messinian-Pliocene section of Cuevas del Almanzora (Vera Basin, SE Spain) revisited-erosional features and strontium isotope ages," *Sedimentary Geology*, vol. 97, no. 3-4, pp. 177–201, 1995.

[25] E. Di Stefano, R. Sprovieri, and S. Scarantino, "Chronology of biostratigraphic events at the base of the Pliocene," *Paleopelagos*, vol. 6, pp. 401–414, 1996.

[26] F. Sgarrella, R. Sprovierp, E. Di Stefano, and A. Caruso, "Paleoceanographic conditions at the base of the Pliocene in the Southern Mediterranean Basin," *Rivista Italiana di Paleontologia e Stratigrafia*, vol. 103, no. 2, pp. 207–220, 1997.

[27] S. Spezzaferri, M. B. Cita, and J. A. McKenzie, "The Miocene—Pliocene boundary in the eastern Mediterranean: results from ODP Leg 160, Sites 967 and 969," in *Proceedings of the Ocean Drilling Program Scientific Results*, A. H. F. Robertson, K.-C. Emeis, C. Richter, and A. Camerlenghi, Eds., vol. 160, pp. 9–28, 1998.

[28] S. Iaccarino, D. Castradori, M. B. Cita et al., "The Miocene/Pliocene boundary and the significance of the earliest Pliocene flooding in the Mediterranean," *Memorie della Società Geologica Italiana*, vol. 54, pp. 109–131, 1999.

[29] S. M. Iaccarino, M. B. Cita, S. Gaboardi, and G. M. Gruppini, "High-resolution biostratigraphy at the Miocene/Pliocene boundary in Holes 974B and 975B, Western Mediterranean," in *Proceedings of the Ocean Drilling Program Scientific Results*, R. Zahn, M. C. Comas, and A. Klaus, Eds., vol. 161, pp. 197–221, 1999.

[30] S. M. Iaccarino and A. Bossio, "Paleoenvironment of uppermost Messinian sequences in the western Mediterranean (sites 974, 975 and 978)," in *Proceedings of the Ocean Drilling Program Scientific Results*, R. Zahn, M. C. Comas, and A. Klaus, Eds., vol. 161, pp. 529–540, 1999.

[31] E. Di Stefano, M. B. Cita, S. Spezzaferri, and R. Sprovieri, "The Messinian-Zanclean Pissouri Section (Cyprus, eastern Mediterranean)," *Memorie della Società Geologica Italiana*, vol. 118, pp. 133–144, 1999.

[32] F. Sgarrella, R. Sprovieri, E. Di Stefano, A. Caruso, M. Sprovieri, and G. Bonaduce, "The Capo Rossello bore-hole (Agrigento, Sicily): cyclostratigraphic and paleoceanographic reconstructions from quantitative analyses of the Zanclean foraminiferal assemblages," *Rivista Italiana di Paleontologia e Stratigrafia*, vol. 105, no. 2, pp. 303–322, 1999.

[33] C. Pierre, A. Caruso, M. M. Blanc-Valleron, J. M. Rouchy, and F. Orzsag-Sperber, "Reconstruction of the paleoenvironmental changes around the Miocene-Pliocene boundary along a West-East transect across the Mediterranean," *Sedimentary Geology*, vol. 188-189, pp. 319–340, 2006.

[34] E. Van Der Laan, E. Snel, E. De Kaenel, F. J. Hilgen, and W. Krijgsman, "No major deglaciation across the Miocene-Pliocene boundary: integrated stratigraphy and astronomical tuning of the Loulja sections (Bou Regreg area, NW Morocco)," *Paleoceanography*, vol. 21, no. 3, Article ID PA3011, 2006.

[35] C. Pierre, J. M. Rouchy, and M. M. Blanc-Valleron, "Sedimentological and stable isotope changes at the Messinian/Pliocene boundary in the eastern Mediterranean Holes 968A, 969A, and 969B," *Proceedings of the Ocean Drilling Program: Scientific Results*, vol. 160, pp. 3–8, 1998.

[36] J. Aguirre and I. M. Sánchez-Almazo, "The Messinian post-evaporitic deposits of the Gafares area (Almería-Níjar basin, SE Spain). A new view of the "Lago-Mare" facies," *Sedimentary Geology*, vol. 168, no. 1-2, pp. 71–95, 2004.

[37] J. C. Braga, J. M. Martín, R. Riding, J. Aguirre, I. M. Sánchez-Almazo, and J. Dinarès-Turell, "Testing models for the Messinian salinity crisis: the Messinian record in Almería, SE Spain," *Sedimentary Geology*, vol. 188-189, pp. 131–154, 2006.

[38] G. Carnevale, W. Landini, and G. Sarti, "Mare versus Largo-mare: marine fishes and the Mediterranean environment at the end of the Messinian Salinity Crisis," *Journal of the Geological Society*, vol. 163, no. 1, pp. 75–80, 2006.

[39] F. Bache, J. L. Olivet, C. Gorini et al., "Messinian erosional and salinity crises: view from the Provence Basin (Gulf of Lions, Western Mediterranean)," *Earth and Planetary Science Letters*, vol. 286, no. 1-2, pp. 139–157, 2009.

[40] F. Bache, S.-M. Popescu, M. Rabineau et al., "A two-step process for the reflooding of the Mediterranean after the Messinian Salinity Crisis," *Basin Research*, vol. 24, pp. 125–153, 2012.

[41] S. M. Popescu, F. Dalesme, G. Jouannic et al., "Galeacysta etrusca complex, dinoflagellate cyst marker of Paratethyan influxes into the Mediterranean Sea before and after the peak of the Messinian Salinity Crisis," *Palynology*, vol. 33, no. 2, pp. 105–134, 2009.

[42] F. J. Hilgen, L. Bissoli, S. Iaccarino et al., "Integrated stratigraphy and astrochronology of the Messinian GSSP at Oued Akrech (Atlantic Morocco)," *Earth and Planetary Science Letters*, vol. 182, no. 3-4, pp. 237–251, 2000.

[43] F. J. Hilgen, W. Krijgsman, I. Raffi, E. Turco, and W. J. Zachariasse, "Integrated stratigraphy and astronomical calibration of the Serravallian/Tortonian boundary section at Monte Gibliscemi (Sicily, Italy)," *Marine Micropaleontology*, vol. 38, no. 3-4, pp. 181–211, 2000.

[44] N. J. Shackleton and S. Crowhurst, "Sediment fluxes based on orbital tuned time scale 5 Ma to 14 Ma, Site 926," in *Proceedings of the Ocean Drilling Program Scientific Results*, N. J. Shackleton, W. B. Curry et al., Eds., vol. 154, pp. 69–82, 1997.

[45] F. J. Sierro, F. J. Hilgen, W. Krijgsman, and J. A. Flores, "The Abad composite (SE Spain): a Messinian reference section for the Mediterranean and the APTS," *Palaeogeography, Palaeoclimatology, Palaeoecology*, vol. 168, no. 1-2, pp. 141–169, 2001.

[46] F. J. Sierro, J. A. Flores, G. Francés et al., "Orbitally-controlled oscillations in planktic communities and cyclic changes in western Mediterranean hydrography during the Messinian," *Palaeogeography, Palaeoclimatology, Palaeoecology*, vol. 190, pp. 289–316, 2003.

[47] L. Vidal, T. Bickert, G. Wefer, and U. Röhl, "Late Miocene stable isotope stratigraphy of SE Atlantic ODP Site 1085: relation to Messinian events," *Marine Geology*, vol. 180, no. 1–4, pp. 71–85, 2002.

[48] W. Krijgsman, S. Gaboardi, F. J. Hilgen, S. Iaccarino, E. De Kaenel, and E. van der Laan, "Revised astrochronology for the

Ain el Beida section (Atlantic Morocco): no glacio-eustatic control for the onset of the Messinian salinity crisis," *Stratigraphy*, vol. 1, no. 1, pp. 87–101, 2004.

[49] J. C. Larrasoaña, J. A. González-Delgado, J. Civis, F. J. Sierro, G. Alonso-Gavilán, and J. Pais, "Magnetobiostratigraphic dating and environmental magnetism of Late Neogene marine sediments recovered at the Huelva-1 and Montemayor-1 boreholes (lower Guadalquivir basin, Spain)," *Geo-Temas*, vol. 10, pp. 1175–1178, 2008.

[50] J. N. Pérez-Asensio, J. Aguirre, G. Schmiedl, and J. Civis, "Messinian paleoenvironmental evolution in the lower Guadalquivir Basin (SW Spain) based on benthic foraminifera," *Palaeogeography, Palaeoclimatology, Palaeoecology*, vol. 326–328, pp. 135–151, 2012.

[51] J. N. Pérez-Asensio, J. Aguirre, G. Schmiedl, and J. Civis, "Impact of restriction of the Atlantic-Mediterranean gateway on the Mediterranean Outflow Water and eastern Atlantic circulation during the Messinian," *Paleoceanography*, vol. 27, 2012.

[52] F. J. Hilgen and W. Krijgsman, "Cyclostratigraphy and astrochronology of the Tripoli diatomite formation (pre-evaporite Messinian, Sicily, Italy)," *Terra Nova*, vol. 11, no. 1, pp. 16–22, 1999.

[53] L. J. Lourens, A. Antonarakou, F. J. Hilgen, A. A. M. Van Hoof, C. Vergnaud-Grazzini, and W. J. Zachariasse, "Evaluation of the Plio-Pleistocene astronomical timescale," *Paleoceanography*, vol. 11, no. 4, pp. 391–413, 1996.

[54] F. J. Hilgen, "Astronomical calibration of Gauss to Matuyama sapropels in the Mediterranean and implication for the Geomagnetic Polarity Time Scale," *Earth and Planetary Science Letters*, vol. 104, no. 2–4, pp. 226–244, 1991.

[55] F. J. Hilgen, "Extension of the astronomically calibrated (polarity) time scale to the Miocene/Pliocene boundary," *Earth and Planetary Science Letters*, vol. 104, pp. 211–225, 1991.

[56] L. Lourens, F. Hilgen, N. J. Shackleton, J. Laskar, and J. Wilson, "Orbital tuning calibrations and conversions for the Neogene Period," in *A Geological Timescale 2004*, F. Gradstein, J. Ogg, and A. Smith, Eds., pp. 469–484, Cambridge University Press, Cambridge, UK, 2004.

[57] N. J. Shackleton, J. G. Baldauf, J. A. Flores, T. C. Moore, I. Raffi, and E. Vincent, "Biostratigraphic summary for LEG 138," in *Proceedings of the Ocean Drilling Program Scientific Results*, N. G. Pias, L. A. Mayer, T. R. Janecek et al., Eds., vol. 138, pp. 517–533, 1995.

[58] F. J. Hilgen, H. Abdul Aziz, W. Krijgsman, I. Raffi, and E. Turco, "Integrated stratigraphy and astronomical tuning of the Serravallian and lower Tortonian at Monte dei Corvi (Middle-Upper Miocene, northern Italy)," *Palaeogeography, Palaeoclimatology, Palaeoecology*, vol. 199, no. 3-4, pp. 229–264, 2003.

[59] F. Hilgen, H. Brinkhuis, and W. J. Zachariasse, "Unit stratotypes for global stages: the Neogene perspective," *Earth-Science Reviews*, vol. 74, no. 1-2, pp. 113–125, 2006.

[60] S. K. Hüsing, F. J. Hilgen, H. Abdul Aziz, and W. Krijgsman, "Completing the Neogene geological time scale between 8.5 and 12.5 Ma," *Earth and Planetary Science Letters*, vol. 253, no. 3-4, pp. 340–358, 2007.

[61] F. J. Hilgen, H. Abdul Aziz, W. Krijgsman et al., "Present status of the astronomical (polarity) time-scale for the Mediterranean Late Neogene," *Philosophical Transactions of the Royal Society A*, vol. 357, no. 1757, pp. 1931–1947, 1999.

[62] R. Sprovieri, "Mediterranean Pliocene biochronology: an high resolution record based on quantitative planktonic foraminifera distribution," *Rivista Italiana di Paleontologia e Stratigrafia*, vol. 98, no. 1, pp. 61–100, 1992.

[63] R. Sprovieri, "Pliocene-early Pleistocene astronomically forced planktonic foraminifera abundance fluctuations and chronology of Mediterranean calcareous plankton bio-events," *Rivista Italiana di Paleontologia e Stratigrafia*, vol. 99, no. 3, pp. 371–414, 1993.

[64] A. Caruso, "Climatic Change During Upper Pliocene/Lower Pleistocene at Capo Rossello (Sicily, Italy): a planktic foraminifers approach," in *Proceedings of the 1st Italian Meeting on Environmental Micropaleontology: Grybowski Foundation Special Pubblication*, R. Coccioni, S. Galeotti, and F. Lirer, Eds., vol. 9, pp. 17–36, 2004.

[65] F. Riforgiato, L. M. Foresi, M. Aldinucci et al., "Foraminiferal record and astronomical cycles: an example from the Messinian pre-evaporitic Gello composite section (Tuscany, Italy)," *Stratigraphy*, vol. 5, no. 3-4, pp. 265–280, 2008.

[66] F. Riforgiato, L. M. Foresi, A. Di Stefano et al., "The Miocene/Pliocene boundary in the Mediterranean area: new insights from a high-resolution micropalaeontological and cyclostratigraphical study (Cava Serredi section, Central Italy)," *Palaeogeography, Palaeoclimatology, Palaeoecology*, vol. 305, no. 1–4, pp. 310–328, 2011.

[67] C. Brunner, J. Sblendorio-Levy, R. Maniscalco et al., "Biostratigraphic and Magnetostratigraphic evaluation of Sites 953, 954, 955, and 956, Canary Islands," in *Proceedings of the Ocean Drilling Program Initial Reports*, P. P. E. Weaver, H.-U. Schmincke, J. V. Firth, and W. Duffield, Eds., vol. 157, pp. 97–114, 1998.

[68] R. Maniscalco and C. A. Brunner, "Neogene and Quaternary planktonic foraminiferal biostratigraphy of the Canary Island region," in *Proceedings of the Ocean Drilling Program Initial Reports* , P. P. E. Weaver, H.-U. Schmincke, J. V. Firth, and W. Duffield, Eds., vol. 157, pp. 115–124, 1998.

[69] "Shipboard Scientific Party, Site 953," in *Proceedings of the Ocean Drilling Program Initial Reports*, H.-U. Schminke, P. P. E. Weaver, J. V. Firth et al., Eds., vol. 157, pp. 317–394, 1995.

[70] H.-U. Schmincke, P. P. E. Weaver, and J. V. Firth, *Proceedings of the Ocean Drilling Program Initial Reports*, vol. 157, ODP, College Station, Tex, USA, 1995.

[71] T. J. Kouwenhoven, C. Morigi, A. Negri, S. Giunta, W. Krijgsman, and J. M. Rouchy, "Paleoenvironmental evolution of the eastern Mediterranean during the Messinian: constraints from integrated microfossil data of the Pissouri Basin (Cyprus)," *Marine Micropaleontology*, vol. 60, no. 1, pp. 17–44, 2006.

[72] F. Rögl and H. M. Bolli, "Holocene to Pleistocene planktonic foraminifera of Leg 15, Site 147 (Cariaco Basin (Trench), Caribbean Sea) and their climatic interrelation," *Initial Reports of the Deep Sea Drilling Project*, vol. 15, pp. 553–615, 1973.

[73] M. M. Blanc-Valleron, C. Pierre, J. P. Caulet et al., "Sedimentary, stable isotope and micropaleontological records of paleoceanographic change in the Messinian Tripoli Formation (sicily, Italy)," *Palaeogeography, Palaeoclimatology, Palaeoecology*, vol. 185, no. 3-4, pp. 255–286, 2002.

[74] M. Pérez-Folgado, F. J. Sierro, M. A. Bárcena et al., "Western versus eastern Mediterranean paleoceanographic response to astronomical forcing: a high-resolution microplankton study of precession-controlled sedimentary cycles during the Messinian," *Palaeogeography, Palaeoclimatology, Palaeoecology*, vol. 190, pp. 317–334, 2003.

[75] W. J. Zachariasse, "Planktonic foraminiferal biostratigraphy of the Late Neogene of Crete (Greece)," *Utrecht Micropaleontology Bulletin*, vol. 11, 1975.

[76] C. Montenat, G. Bizon, and J. J. Bizon, "Continuité ou discontinuité de sédimentation marine mio-pliocène en Méditerranée occidentale. L'exemple du bassin de Vera (Espagne méridionale)," *Revue de l'Institut Français du Pétrole*, vol. 31, pp. 613–663, 1976.

[77] J. Civis, J. Martinell, and J. de Porta, "Microfauna del Mioceno terminal de la Rambla de Arejos (Almeria)," *Studia Geologica*, vol. 15, pp. 37–55, 1979.

[78] M. L. Colalongo, A. Di-Grande, S. D'Onofrio et al., "Stratigraphy of Late Miocene Italian sections straddling the Tortonian/Messinian boundary," *Bollettino della Società Paleontologica Italiana*, vol. 18, no. 2, pp. 258–302, 1979.

[79] S. Iaccarino and G. Salvatorini, "A framework of planktonic foraminiferal biostratigraphy for Early Miocene to Late Pliocene Mediterranean area," *Paleontologia Stratigrafica ed Evoluzione, Quad*, vol. 2, pp. 115–125, 1982.

[80] S. Iaccarino, "Mediterranean Miocene and Pliocene planktic foraminifera," in *Plankton Stratigraphy*, H. M. Bolli, J. B. Saunders, and K. Perch-Nielsen, Eds., pp. 283–314, Cambridge University Press, New York, NY, USA, 1985.

[81] H. M. Van De Poel, "Messinian stratigraphy of the Nijar Basin, (S.E. Spain) and the origin of its gypsum-ghost limestones," *Geologie en Mijnbouw*, vol. 70, no. 3, pp. 215–234, 1991.

[82] F. J. Sierro, J. A. Flores, J. Civis, J. A. González Delgado, and G. Francés, "Late Miocene globorotaliid event-stratigraphy and biogeography in the NE-Atlantic and Mediterranean," *Marine Micropaleontology*, vol. 21, no. 1–3, pp. 143–167, 1993.

[83] F. J. Sierro, J. A. Flores, I. Zamarreño et al., "Astronomical cyclicity and sapropels in the pre-evaporitic Messinian of the Sorbas Basin (Western Mediterranean)," *Geogaceta*, vol. 21, pp. 131–134, 1997.

[84] F. Gautier, G. Clauzon, J. P. Suc, J. Cravatte, and D. Violanti, "Age and duration of the Messinian salinity crisis," *Comptes Rendus—Academie des Sciences, Serie II*, vol. 318, no. 8, pp. 1103–1109, 1994.

[85] R. Sprovieri, E. Di Stefano, A. Caruso, and S. Bonomo, "High resolution stratigraphy in the Messinian Tripoli Formation in Sicily," *Paleopelagos*, vol. 6, pp. 415–435, 1996.

[86] R. Sprovieri, E. Di Stefano, and M. Sprovieri, "High resolution chronology for late miocene mediterranean stratigraphic events," *Rivista Italiana di Paleontologia e Stratigrafia*, vol. 102, no. 1, pp. 77–104, 1996.

[87] H. Feinberg and H. G. Lorenz, "Nouvelles données stratigraphiques su le Miocène superieur et le Pliocène de Maroc-occidental," *Notes et Mémoires du Service Geologique du Maroc*, vol. 30, no. 225, pp. 21–26, 1970.

[88] R. M. Stainforth, J. L. Lamb, H. Luterbacher, J. H. Beard, and R. M. Jeffords, "Cenozoic Planktonic zonation and characteristics of Index forms," *University of Kansas Paleontological Contributions*, vol. 62, 1975.

[89] A. Bossio, K. Rakic El-Beid, L. Giannelli, R. Mazzei, A. Russo, and G. Salvatorini, "Correlation de quelques sections stratigraphiques du Mio-Pliocène de la zone Atlantique du Maroc avec les stratotypes du Bassin Mediterranéen sur la base des Foraminifères planctoniques, Nannoplancton calcaire et Ostracodes," *Atti della Societa Toscana di Scienze Naturali. Memorie*, vol. 83, pp. 121–137, 1976.

[90] M. B. Cita and W. B. F. Ryan, "The Bou Regreg section of the Atlantic coast of Morocco: evidence, timing and significance of a late Miocene regressive phase," *Rivista Italiana di Paleontologia*, vol. 84, pp. 1051–1082, 1978.

[91] R. Mazzei, I. Raffi, D. Rio, N. Hamilton, and M. B. Cita, "Calibration of the late Neogene calcareous plankton datum planes with the paleomagnetic record of Site 397 and correlation with Moroccan and Mediterranean sections," *Initial Reports of the Deep Sea Drilling Project*, vol. 47, no. 1, pp. 375–389, 1979.

[92] G. Salvatorini and M. B. Cita, "Miocene foraminiferal stratigraphy, DSDP Site 397 (Cape Bojador, North Atlantic)," *Initial Reports of the Deep Sea Drilling Project*, vol. 47, pp. 317–373, 1979.

[93] F. J. Sierro, *Foraminiferos planctónicos y bioestratigrafia del Mioceno superior-Plioceno del borde occidental de la cuenca del Guadalquivir (SO de España) [dissertation]*, Universidad de Salamanca, 1984.

[94] D. A. Hodell, R. H. Benson, J. P. Kennett, and K. Rakic-El Bied, "Stable isotope stratigraphy of latest Miocene sequences in northwest Morocco: the Bou Regreg Section," *Paleoceanography*, vol. 4, no. 4, pp. 467–482, 1989.

[95] D. A. Hodell, J. H. Curtis, F. J. Sierro, and M. E. Raymo, "Correlation of late Miocene to early Pliocene sequences between the Mediterranean and North Atlantic," *Paleoceanography*, vol. 16, no. 2, pp. 164–178, 2001.

[96] R. H. Benson, K. Rakic-El Bied, and G. Bonaduce, "An important current reversal (influx) in the Rifian Corridor (Morocco) at the Tortonian-Messinian boundary: the end of Tethys Ocean," *Paleoceanography*, vol. 6, no. 1, pp. 165–192, 1991.

[97] R. H. Benson, L. A. C. Hayek, D. A. Hodell, and K. Rakic-El Bied, "Extending the climatic precession curve back into the late Miocene by signature template comparison," *Paleoceanography*, vol. 10, no. 1, pp. 5–20, 1995.

[98] R. H. Benson and K. Rakic-El Bied, "The Bou Regreg section, Morocco: proposed global boundary stratotype section and point of the Pliocene," *Notes et Mémoires du Service Géologique*, vol. 383, pp. 51–150, 1996.

[99] J. Zhang and D. B. Scott, "Integrated stratigraphy and paleoceanography of the Messinian (latest Miocene) across the North Atlantic Ocean," *Marine Micropaleontology*, vol. 29, no. 1, pp. 1–36, 1996.

[100] C. Morigi, A. Negri, S. Giunta et al., "Integrated quantitative biostratigraphy of the latest Tortonian-early Messinian Pissouri section (Cyprus): an evaluation of calcareous plankton bioevents," *Geobios*, vol. 40, no. 3, pp. 267–279, 2007.

[101] D. A. Hodell, R. H. Benson, D. V. Kent, A. Boersma, and K. Rakic-El Bied, "Magnetostratigraphic, biostratigraphic, and stable isotope stratigraphy of an Upper Miocene drill core from the Sale Briqueterie (northwestern Morocco): a high-resolution chronology for the Messinian stage," *Paleoceanography*, vol. 9, no. 6, pp. 835–855, 1994.

[102] W. Krijgsman, M. M. Blanc-Valleron, R. Flecker et al., "The onset of the Messinian salinity crisis in the Eastern Mediterranean (Pissouri Basin, Cyprus)," *Earth and Planetary Science Letters*, vol. 194, no. 3-4, pp. 299–310, 2002.

[103] P. W. P. Hooper and P. P. E. Weaver, "Paleoceanographic significance of late Miocene to early Pliocene planktonic foraminifers at Deep Sea Drilling Project Site 609," *Initial Reports of the Deep Sea Drilling Project*, vol. 94, no. 2, pp. 925–934, 1987.

[104] J. Laskar, P. Robutel, F. Joutel, M. Gastineau, A. C. M. Correia, and B. Levrard, "A long-term numerical solution for the insolation quantities of the Earth," *Astronomy and Astrophysics*, vol. 428, no. 1, pp. 261–285, 2004.

[105] F. J. Sierro, "The replacement of the "Globorotalia menardii" group by the Globorotalia miotumida group: an aid to recognizing the Tortonian-Messinian boundary in the Mediterranean and adjacent Atlantic," *Marine Micropaleontology*, vol. 9, no. 6, pp. 525–535, 1985.

[106] F. J. Sierro, J. A. Flores, J. Civis, and J. A. González-Delgado, "New criteria for the correlation of the Andalusian and Messinian stages," *Annales. Instituti Geologici Publici Hungarici*, vol. 70, pp. 355–361, 1987.

[107] J. A. Flores and F. J. Sierro, "Calcareous nannoflora and planktonic foraminifera in the Tortonian/Messinian boundary interval of East Atlantic DSDP Sites and their relation to Spanish and Morroccan sections," in *Nannofossils and Their Applications*, S. E. van Heck and J. Crux, Eds., British Micropaleontological Society Series, pp. 249–266, 1989.

[108] R. Z. Poore, "Tertiary Oligocene through Quaternary planktonic foraminiferal biostratigraphy of the North Atlantic: DSDP Leg 49," *Initial Reports of the Deep Sea Drilling Project*, vol. 49, pp. 447–518, 1979.

[109] M. B. Cita, "Mediterranean evaporite: paleontological arguments for a deep-basin desiccation model," in *Messinian Events in the Mediterranean*, C. W. Drooger, Ed., pp. 206–228, North-Holland, Amsterdam, The Netherland, 1973.

[110] M. B. Cita, "Planktonic foraminiferal biozonation of the Mediterranean Pliocene deep sea record. A revision Studi sul Pliocene e sugli strati di passaggio dal Miocene al Pliocene," *Rivista Italiana di Paleontologia*, vol. 81, pp. 527–544, 1975.

[111] M. B. Cita, "Planktonic foraminiferal biostratigraphy of the Mediterranean Neogene," in *Progress in Micropaleontology, Special Pubblications*, Y. Takayanagi and T. Saito, Eds., pp. 47–68, Micropaleontology Press, 1976.

[112] H. M. Bolli and J. B. Saunders, "Oligocene to Holocene low latitude planktic foraminifera," in *Plankton Stratigraphy*, H. M. Bolli, J. B. Saunders, and K. Perch-Nielsen, Eds., pp. 283–314, Cambridge University Press, 1985.

[113] C. G. Langereis and F. J. Hilgen, "The Rossello composite: a Mediterranean and global reference section for the Early to early Late Pliocene," *Earth and Planetary Science Letters*, vol. 104, no. 2–4, pp. 211–225, 1991.

[114] W. A. Berggren, "Late Neogene planktonic foraminiferal biostratigraphy of DSDP Site 357 (Rio Grande Rise)," in *Initial Reports of the Deep Sea Drilling Project*, P. R. Supko, K. Perch-Nielsen, R. L. Carlson et al., Eds., vol. 12, pp. 965–1001, 1977.

[115] W. A. Berggren, D. V. Kent, and J. A. van Couvering, "Neogene geochronology and chronostratigraphy," in *The Chronology of the Geologic Record, the Neogene: Part 2*, pp. 211–259, Blackwell Science, 1985.

[116] M. S. Srinivasan and J. P. Kennett, "A review of Neogene planktonic foraminiferal biostratigraphy and evolution: applications in the Equatorial and South Pacific," *Special Publications of SEPM*, vol. 32, pp. 395–492, 1981.

[117] M. S. Srinivasan and J. P. Kennett, "Neogene planktonic foraminiferal biostratigraphy and evolution: equatorial to subantarctic, South Pacific," *Marine Micropaleontology*, vol. 6, no. 5-6, pp. 499–533, 1981.

[118] J. P. Kennett, "Middle and Late Cenozoic planktonic foraminiferal biostratigraphy of the Southwest Pacific-DSDP Leg 21," in *Initial Reports of the Deep Sea Drilling Project*, E Burns, J. E. Andrews, and G. J. van der Lingen, Eds., vol. 21, pp. 575–639, 1973.

[119] P. P. E. Weaver and H. Bergsten, "Assessing the accuracy of fossil datum levels: *Globorotalia margaritae* Foraminiferida, a Pliocene test case," *Journal of Micropalaeontology*, vol. 9, no. 2, pp. 225–231, 1990.

[120] T. Saito, L. H. Burckle, and J. D. Hays, "Late Miocene to Pleistocene biostratigraphy of equatorial Pacific sediments," in *Late Neogene Epoch Boundaries*, pp. 226–244, Micropaleontology Press, 1975.

[121] I. Raffi and J. A. Flores, "Pleistocene through Miocene calcareous nannofossils from eastern equatorial Pacific Ocean (Leg 138)," in *Proceedings of the Ocean Drilling Program Science Results*, vol. 138, pp. 233–286, 1995.

[122] I. Raffi, D. Rio, A. D'Atri, E. Fornaciari, and S. Rocchetti, "Quantitative distribution patterns and biomagnetostratigraphy of Middle and Late Miocene calcareous nannofossils from equatorial Indian and Pacific Ocean," in *Proceedings of the Ocean Drilling Program Science Results*, vol. 138, pp. 79–502, 1995.

[123] J. Backman and I. Raffi, "Calibration of Miocene nannofossil events to orbitally tuned cyclostratigraphies from Ceara Rise," *Proceedings of the Ocean Drilling Program Science Results*, vol. 154, pp. 83–99, 1997.

[124] I. Raffi, J. Backman, E. Fornaciari et al., "A review of calcareous nannofossil astrobiochronology encompassing the past 25 million years," *Quaternary Science Reviews*, vol. 25, no. 23-24, pp. 3113–3137, 2006.

[125] H. Okada and D. Bukry, "Supplementary modification and introduction of code numbers to the low-latitude coccolith biostratigraphic zonation (Bukry, 1973; 1975)," *Marine Micropaleontology*, vol. 5, pp. 321–325, 1980.

[126] D. Rio, R. Sprovieri, and I. Raffi, "Calcareous plankton biostratigraphy and biochronology of the Pliocene-Lower Pleistocene succession of the Capo Rossello area, Sicily," *Marine Micropaleontology*, vol. 9, no. 2, pp. 135–180, 1984.

[127] R. Thunell, D. Rio, R. Sprovieri, and I. Raffi, "Limestone-marl couplets: origin of the early Pliocene Trubi Marls in Calabria, southern Italy," *Journal of Sedimentary Petrology*, vol. 61, no. 7, pp. 1109–1122, 1991.

[128] R. Thunell, D. Rio, R. Sprovieri, and C. Vergnaud-Grazzini, "An overview of the post-Messinian paleoenvironmental history of the western Mediterranean," *Paleoceanography*, vol. 6, no. 1, pp. 143–163, 1991.

[129] A. Di Stefano and G. Sturiale, "Refinements of calcareous nannofossil biostratigraphy at the Miocene/Pliocene Boundary in the Mediterranean region," *Geobios*, vol. 43, no. 1, pp. 5–20, 2010.

[130] J. A. Van Couvering, D. Castradori, M. B. Cita, F. J. Hilgen, and D. Rio, "The base of the Zanclean Stage and of the Pliocene series," *Episodes*, vol. 23, no. 3, pp. 179–187, 2000.

[131] A. Caruso, M. Sprovieri, A. Bonanno, and R. Sprovieri, "Astronomical calibration of the Serravallian/Tortonian Case Pelacani section (Sicily, Italy)," *Rivista Italiana di Paleontologia e Stratigrafia*, vol. 108, no. 2, pp. 297–306, 2002.

[132] M. Sprovieri, A. Caruso, L. M. Foresi et al., "Astronomical calibration of the upper Langhian/lower Serravallian record of Ras il-Pellegrin section (Malta Island, Central Mediterranean)," *Rivista Italiana di Paleontologia e Stratigrafia*, vol. 108, no. 2, pp. 183–193, 2002.

[133] M. Sprovieri, A. Bellanca, A. Neri et al., "Astronomical calibration of late Miocene stratigraphic events and analysis of precessionally driven paleoceanographic changes in the Mediterranean basin," *Memorie della Società Geologica Italiana*, vol. 54, pp. 7–24, 1999.

[134] A. Bellanca, A. Caruso, G. Ferruzza et al., "Transition from marine to hypersaline conditions in the Messinian Tripoli Formation from the marginal areas of the central Sicilian Basin," *Sedimentary Geology*, vol. 140, no. 1-2, pp. 87–105, 2001.

[135] A. Vázquez, R. Utrilla, I. Zamarreño et al., "Precession-related sapropelites of the Messinian Sorbas Basin (South Spain): paleoenvironmental significance," *Palaeogeography, Palaeoclimatology, Palaeoecology*, vol. 158, no. 3-4, pp. 353–370, 2000.

[136] A. W. H. Bé, "An ecological, zoogeographic and taxonomic review of recent planktonic foraminifers," in *Oceanic Micropaleontology*, A. T. S. Ramsey, Ed., pp. 1–101, Academic Press, New York, NY, USA, 1977.

[137] B. Luz and Z. Reiss, "Stable carbon isotopes in Quaternary foraminifers from the Gulf of Aqaba (Etlat), Red Sea," *Utrech Micropaleontological Bulletins*, vol. 30, pp. 129–140, 1983.

[138] C. Pujol and C. V. Grazzini, "Distribution patterns of live planktic foraminifers as related to regional hydrography and productive systems of the Mediterranean Sea," *Marine Micropaleontology*, vol. 25, no. 2-3, pp. 187–217, 1995.

[139] R. G. Fairbanks and P. H. Wiebe, "Foraminifera and chlorophyll maximum: vertical distribution, seasonal succession, and paleoceanographic significance," *Science*, vol. 209, no. 4464, pp. 1524–1526, 1980.

[140] R. G. Fairbanks, M. Sverdlove, R. Free, P. H. Wiebe, and A. W. H. Bé, "Vertical distribution and isotopic fractionation of living planktonic foraminifera from the Panama Basin," *Nature*, vol. 298, no. 5877, pp. 841–844, 1982.

[141] E. J. Rohling and W. W. C. Gieskes, "Late Quaternary changes in Mediterranean intermediate water density and formation rate," *Paleoceanography*, vol. 4, no. 5, pp. 531–545, 1989.

[142] F. J. Sierro, J. A. Flores, I. Zamarreño et al., "Messinian pre-evaporite sapropels and precession-induced oscillations in western Mediterranean climate," *Marine Geology*, vol. 153, no. 1–4, pp. 137–146, 1999.

[143] A. W. H. Bé and D. S. Tolderlund, "Distribution and ecology of living planktonic foraminifera in surface waters of the Atlantic and Indian Oceans," in *The Micropaleontology of Oceans*, B. M. Funnel and W. R. Riedel, Eds., pp. 105–149, Cambridge University Press, London, UK, 1971.

[144] C. Hemleben, M. Spindler, and O. R. Anderson, *Modern Planktonic Foraminifera*, Springer, New York, NY, USA, 1989.

[145] A. W. H. Bé, G. Vilks, and I. Lott, "Winter distribution of planktonic foraminifera between the Grand Banks and the Caribbean," *Micropaleontology*, vol. 17, pp. 31–42, 1971.

[146] R. J. W. Van Leeuwen, "Sea-floor distribution and Late Quaternary faunal patterns of planktonic and benthic foraminifers in the Angola Basin," *Utrecht Micropaleontological Bulletins*, vol. 38, p. 287, 1989.

[147] B. Malmgren and J. P. Kennett, "Biometric analyses of phenotypic variation: *Globigerina bulloides* and *Globigerina falconensis* in the southern Indian Ocean," *Journal of Foraminiferal Research*, vol. 7, pp. 130–148, 1977.

[148] W. Krijgsman, F. J. Hilgen, A. Negri, J. R. Wijbrans, and W. J. Zachariasse, "The Monte del Casino section (Northern Apennines, Italy): a potential Tortonian/Messinian boundary stratotype?" *Palaeogeography, Palaeoclimatology, Palaeoecology*, vol. 133, no. 1-2, pp. 27–47, 1997.

[149] S. J. Schenau, A. Antonarakou, F. J. Hilgen et al., "Organic-rich layers in the Metochia section (Gavdos, Greece): evidence for a single mechanism of sapropel formation during the past 10 My," *Marine Geology*, vol. 153, no. 1–4, pp. 117–135, 1999.

[150] G. M. Filippelli, F. J. Sierro, J. A. Flores et al., "A sediment-nutrient-oxygen feedback responsible for productivity variations in Late Miocene sapropel sequences of the western Mediterranean," *Palaeogeography, Palaeoclimatology, Palaeoecology*, vol. 190, pp. 335–348, 2003.